THREE-DIMENSIONAL CFD MODELLING OF THE EFFECT OF SOME OPERATING PARAMETERS ON PARTICLE TRAJECTORIES IN A ROTATING FLUIDISED BED COMBUSTOR

M. Rozainee and S. P. Ngo*
Department of Chemical Engineering
Faculty of Chemical Engineering & Natural Resources Engineering
Universiti Teknologi Malaysia
81310 Skudai, Johor

ABSTRACT

The objective of the research was to investigate the trajectories of particles in a horizontal rotating fluidised bed (RFB) combustor. Due to the conservation of momentum, the gases in a RFB are imparted a tangential velocity component which accelerates as they converge to the exit. Dependant upon the type and size of particle, this unique feature causes particles in the RFB to be returned to be bed, be captured and remained in circular orbit in the freeboard region of the primary chamber or be blown out of the combustor. Hence, computational fluid dynamics (CFD) modelling had been performed using the FLUENT program code to chart the trajectory of rice husk ash particles of various sizes in a RFB operated at different rotating speeds and air feed rates. It was found that, in general, particles of size less than 5 μm were rapidly blown out of the combustor while particles in the range of 10 – 50 μm were retained in the primary chamber. Larger-sized particles (>50 μm) tended to move towards the distributor due to higher momentum.

Keywords: computational fluid dynamics; particle trajectory; rotating fluidised bed

INTRODUCTION

A very important feature of the rotating fluidised bed (RFB) is that the gases are imparted a tangential velocity component, which accelerates due to the conservation of momentum as the gases converge towards the exit. Apart from causing unburnt particles to be returned to the bed to complete the combustion process, the swirling effect also increases the residence time of these particles in the freeboard region. Hence, the trajectory of particles such as ash in the RFB presents an interesting field of study as it provides insight as to the elutriation behaviour of these particles. Three-dimensional computational fluid dynamics (CFD) modelling had been performed using the FLUENT program code (version 5.3) to investigate the trajectories of rice husk ash particles of different sizes in a RFB operated at different sets of operating conditions (rotating speeds and air feed rates). FLUENT is a powerful general purpose computer program for modelling fluid flow, heat transfer and chemical reaction. The basic approach utilised is that of solving the conservation equations for mass, momentum, energy and chemical species using a control volume based finite difference method.

DESCRIPTION OF THE RFB TESTING RIG

The RFB rig is a cylindrical chamber mounted horizontally, with the walls of the primary chamber tapered at a certain angle to equalise the non-uniform radial fluidisation inherent in RFB due to the curvature effect (Figure 1).

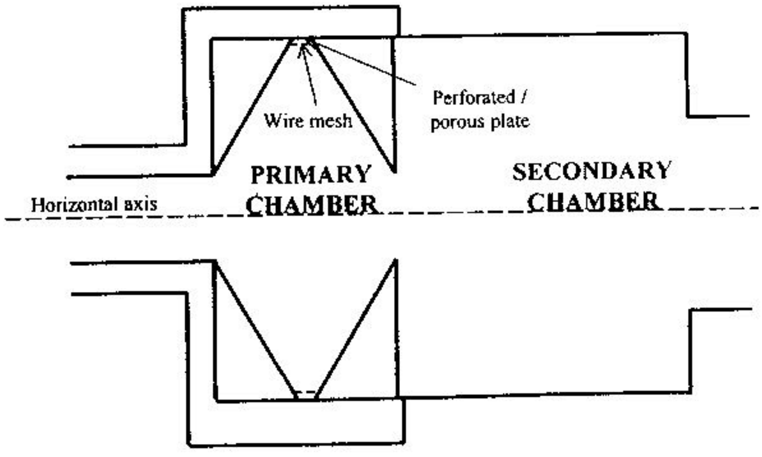

Figure 1: Schematic diagram of the horizontal rotating fluidised bed combustor

The secondary chamber is a hollow cylinder having the same inner diameter as the primary chamber. The whole assembly is rotating on a horizontal axis with high-pressure air being injected into the primary chamber as fluidising fluid. The trajectories of particles, in particular ash particles resulting from the combustion process taking place in the primary chamber, are of research interest in order to predict the retainment of these particles in the bed as well as the level of particulate emissions.

GOVERNING EQUATIONS

Prediction of the isothermal flow field in the computational grid is through solution of the equations for the conservation of mass and momentum in their time averaged form. The set of governing equations for the gas phase was given in Appendix 1.

Equation of Motion for A Particle

FLUENT predicted the trajectory of a discrete phase particle by integrating the force balance on the particle, which is written in a Langrarian reference frame. This force balance equates the particle inertia with the forces acting on the particle, and can be written (for the x direction in Cartesian coordinates) as

$$\frac{du_p}{dt} = F_D(u - u_p) + \frac{g_x(\rho_p - \rho)}{\rho_p} + F_x \tag{1}$$

where $F_D(u - u_p)$ is the drag force per unit particle mass and

$$F_D = \frac{18\mu}{\rho_p D_p^2} \frac{C_D \,\mathrm{Re}}{24} \tag{2}$$

Here, u is the fluid phase velocity, u_p is the particle velocity, μ is the molecular viscosity of the fluid, ρ is the fluid density, ρ_p is the density of the particle, and D_p is the particle diameter. Re is the relative Reynolds number, which is defined as

$$\mathrm{Re} = \frac{\rho D_p |u_p - u|}{\mu} \tag{3}$$

The drag coefficient, C_D is taken from

$$C_D = \frac{24}{\mathrm{Re}}\left(1 + b_1 \mathrm{Re}^{b_2}\right) \frac{b_3 \mathrm{Re}}{b_4 + \mathrm{Re}} \tag{4}$$

where

$b_1 = 2.3288 - 6.4581\phi + 2.4486\phi^2$
$b_2 = 0.0964 + 0.5565\phi$
$b_3 = 4.905 - 13.8944\phi + 18.4222\phi^2 - 10.2599\phi^3$
$b_4 = 1.4681 + 12.2584\phi - 20.7322\phi^2 + 15.8855\phi^3$

which is taken from Haider and Levenspiel [1] for nonspherical particles. The shape factor, ϕ, is given by $\phi = \frac{s}{S}$ where s is the surface area of a sphere having the same volume as the particle, and S is the actual surface area of the particle.

The additional force term, F_x in Equation (1) includes the Coriolis and centrifugal forces acting on the particle arising from the rotational movement of the RFB. The trajectory equations were solved by stepwise integration over discrete time steps. Integration in time of Equation (1) yielded the velocity of the particle at each point along the trajectory, with the trajectory itself predicted by $\frac{dx}{dt} = u_p$, $\frac{dy}{dt} = v_p$ and $\frac{dz}{dt} = w_p$ respectively. The particle phase was assumed to be sufficiently dilute, thus rendering negligible effects on the continuous phase.

NUMERICAL SOLUTION

The RFB Model

The FLUENT computer code (version 5.3) together with calculation data from the equations of fluidisation in a RFB [4] to provide boundary conditions, were used to model the trajectories of particles in a RFB at various operating conditions. Judging from the symmetry in geometry of the RFB and computational efforts, only a quarter of the entire RFB rig was modelled. The boundary conditions at the symmetrical cross sectional area were set as periodic to represent rotational movement (Figure 2). The domain consisted of an unstructured grid of 32 509 cells employing the TGrid meshing scheme, with the axis of rotation set at the *x* direction in the Cartesian coordinates. The flow profiles in the model were first established in an isothermal field, after which ash particles of various sizes were injected and their respective trajectories charted. Air at ambient temperature and certain flow rates consistent with the desired operating conditions entered radially through the distributor plate. However, velocity vectors of the airflow were imparted a tangential component upon entering the porous or perforated distributor plate due to frictional force. The default convergence criteria were that iterations were performed until the scaled residuals decrease to a value of 10^{-3} for all equations (except for energy, whereby the value of 10^{-6} applies but is irrelevant in the present study).

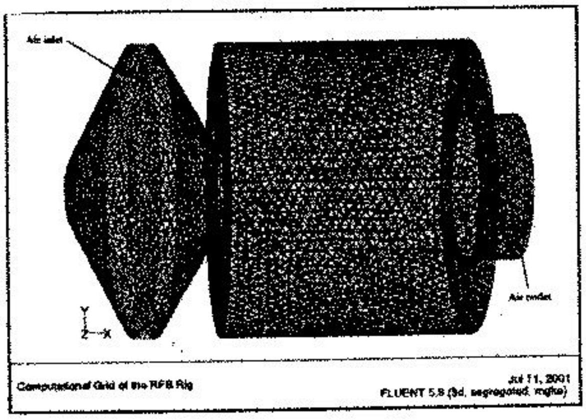

Figure 2: The computational grid of the horizontal RFB rig

Modelling of Particle Trajectory in a RFB Freeboard

Ejection of particles from the bubbling fluidised bed into the freeboard region is the result of bubble eruption on the bed surface. It was reported by Rozainee [4] that the initial velocity of ejected particles is independent of the size and density of the particles, being largely dependant on the size and rise velocity of the bubble [2]. It was further reported that if the ejected particles were from bubble wakes, the particle ejection velocity could be as high as 2.5 times the bubble rise velocity ($V_m = 2.5\ U_b$) [7].

In a RFB, the velocity of bubble swarms can be estimated by the following equation by Subzwari [3]:-

$$U_b = U - U_{mf} + 0.71\,\omega\sqrt{r d_b} \tag{5}$$

where

U_b	=	bubble velocity
U	=	fluidising velocity
U_{mf}	=	minimum fluidising velocity
d_b	=	bubble diameter
r	=	radial position

All parameters for Equation (5) were evaluated at the radial position of the bed surface ($r = r_i$) since the values of fluidising velocity and minimum fluidising velocity in a RFB are dependent upon the radial position. With a bed thickness of 0.15 m made up of 0.725 mm sand in the horizontal RFB combustor (ID = 300 mm) operating at room temperature, the corresponding parameters were evaluated and presented in the following table.

Table 1: Particle ejection velocities at different operating conditions

g-loading	ω (rad/s)	No. of U_{mfc}	U_{mf} (U_{mfs} @ r = r_i)	U (m/s)	U_b (m/s)	2.5 x U_b (m/s)	u_p (m/s)	v_p (m/s)	w_p (m/s)
5	12.79	1	0.24	0.31	0.57	1.41	0	-1.41	1.92
		2		0.62	0.87	2.18	0	-2.18	
		3		0.92	1.18	2.95	0	-2.95	
10	18.08	1	0.41	0.50	0.80	1.99	0	-1.99	2.71
		2		1.01	1.30	3.25	0	-3.25	
		3		1.51	1.81	4.51	0	-4.51	
15	22.15	1	0.55	0.66	0.97	2.43	0	-2.43	3.32
		2		1.32	1.63	4.08	0	-4.08	
		3		1.98	2.29	5.73	0	-5.73	

In estimating the bubble velocity, the bubble diameter was assumed to be 20 mm, a value obtained by Rozainee [4] from his visual observation of the bubbling bed in a Perspex RFB. Consistent with the prediction particle ejection velocity by Pemberton and Davidson [7], the maximum ejected particles velocities at each operating condition was evaluated. The eruption of bubbles was assumed to have ejected the particles in the radial direction only. Therefore, the axial velocity of the ejected particles was assumed to be zero. Also, the ejected particles have a tangential velocity component due to the solid body rotation effect of the rotating beds.

For the sake of tracking their trajectories, the particles were assumed to be ejected singly into the freeboard region. Thereon, the particles were acted upon by the centrifugal force, which tended to return them to the bed. At the same time, the drag force acting in the direction of the gas velocity relative to the particle, tended to bring them towards the centre. In addition, in a frame of reference rotating with the bed, the Coriolis force acted on the particles in such a way as to tend to displace them in a direction normal to their velocity and in the direction of rotation [5].

RESULTS AND DISCUSSION

Effect of Particle Diameter

To study the effect of particle diameters on the trajectories of particles ejected into the freeboard region due to bubble eruption at the bed surface, the horizontal RFB was operated at 15-g loading (211 RPM) and 3 U_{mfc} (5.28 m/s @ room temperature). The particles used were rice husk ash particles having a density of 1590 kg/m^3. The particles were assumed to be ejected from the bed surface of the 150 mm thick bed, mid-length of the primary chamber (x = 150 mm). It was found that, at these operating conditions, the particle trajectories were distinguishable with five particle diameters (5 μm, 10 μm, 25 μm, 50 μm and 1 mm).

As shown in Figure 3, particle with a diameter of 5 μm moved radially inward inside the primary chamber due to high initial radial velocity. High axial velocity at the exit of the primary chamber (as high as 3.76 m/s, Figure 4) then caused the particle to be blown into the secondary chamber, after which it was blown out from the combustor at less than 0.02 s. Particle with a diameter of 10 μm was re-circulating infinitely at regions just after the exit from the primary chamber (Figure 5). Particle of this size was trapped in the re-circulating air flows near the front wall of the secondary chamber of the horizontal RFB (Figure 4). Particles with a diameter of more than 25 μm remained in the primary chamber without entering the secondary chamber. Ash particles with diameters of 25 μm and 50 μm were moving with the swirling flows in the primary chamber in helical trajectories, with the latter having a helical trajectory of larger radius due to higher particle mass (Figure 6 and Figure 7). Particle having a diameter of 1 mm was returned to the bed rapidly due to higher momentum. This phenomenon indicated that at the designated operating conditions, the drag force of the fluid was not sufficient to entrain the particles from the bed surface into the freeboard region.

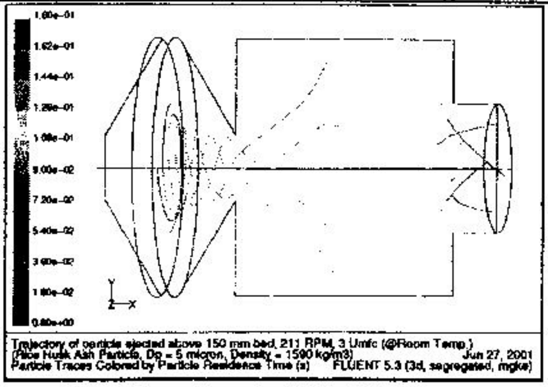

Figure 3: Trajectory of 5 μm ash particle in a RFB operating at 211 RPM, 3 U_{mfc} (@ room temp.)

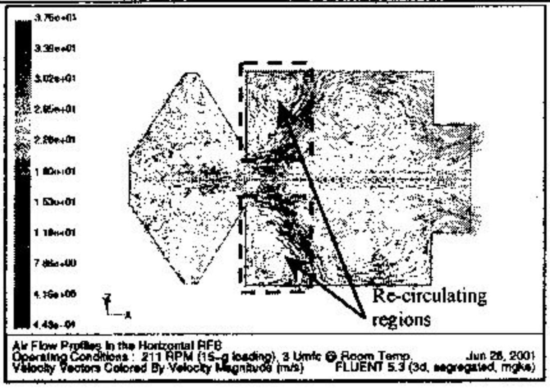

Figure 4: Velocity vectors in a RFB operating at 211 RPM, 3 U_{mfc} (@ room temp.)

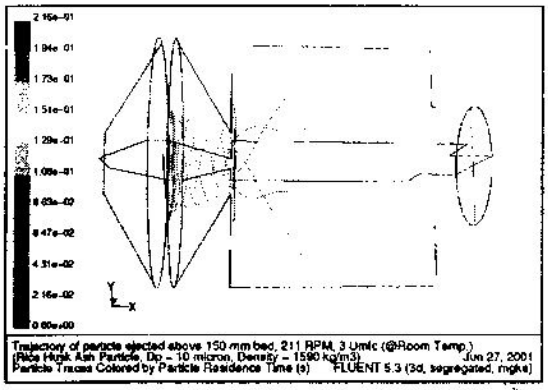

Figure 5: Trajectory of 10 μm ash particle in a RFB operating at 211 RPM, 3 U_{mfc} (@ room temp.)

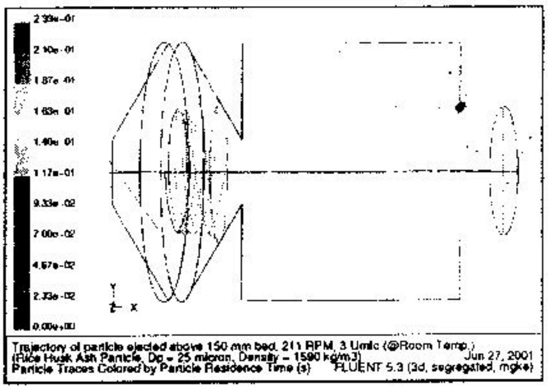

Figure 6: Trajectory of 25 μm ash particle in a RFB operating at 211 RPM, 3 U_{mfc} (@ room temp.)

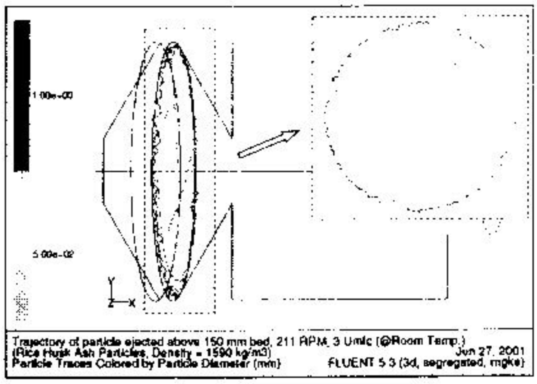

Figure 7: Trajectory of 50 μm and 1 mm ash particles in a RFB operating at 211 RPM, 3 U_{mfc} (@ room temp.)

Effect of rotating speed

The effect of rotating speeds on the trajectories of entrained ash particles was investigated by operating the horizontal RFB at 5-g, 10-g and 15-g loadings with air feed rates held at 3 U_{mfc} accordingly. At these g-loadings, the air feed rates to establish operating conditions of 3 U_{mfc} were 2.46 m/s, 4.02 m/s and 5.28 m/s (at room temperature) respectively. The size of particle chosen was 25 micron as particles of this size were retained in the primary chamber due to the swirling flows. As such, it provided insight as to the effect of changing the rotating speed on the particle residence time in the primary chamber. Besides, another intention was to determine the return of these particles to the bed. Smaller sized particles (5 – 10 μm) were rapidly blown out from the primary chamber into the secondary chamber.

Larger sized particles (> 50 μm), on the other hand, tended to move towards the distributor plate, similar to that observed for particles of 1 mm as in Figure 7.

As expected, the particle residence time decreased as the bed rotating speeds were increased. Increase in bed rotating speeds resulted in higher air feed rates in order to maintain operating conditions of 3 U_{mfc}. Hence, in the present cases, the gas residence time in the primary chamber varies inversely with the bed rotating speed (Figure 8). Although the particle trajectories were quite similar in all three cases (Figure 9 – 11), the residence time in the primary chamber decreased from 0.412 s to 0.292 s and 0.235 s as the rotating speeds were increased from 5-g, 10-g and 15-g loadings respectively. The air feed rates to the primary chamber have to be maintained at a minimum of 3 U_{mfc} to establish turbulence conditions crucial in attaining good mixing behaviour inside the bed. Therefore, it was recommendable that the bed be operated at low rotating speeds in order to increase the particle residence time.

Also apparent was the observation that ejected particles in all three cases were hovering near the surface of the sand bed at a radial position of r = 0.15 m.

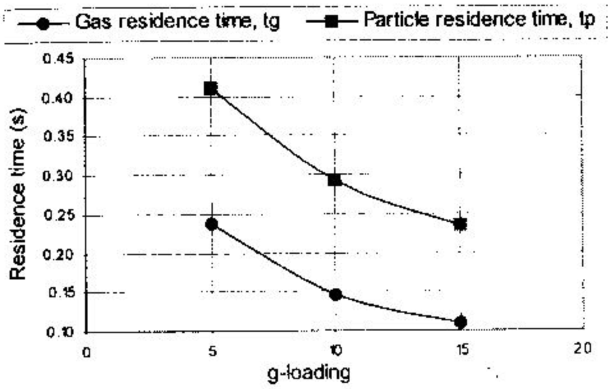

Figure 8: Plot of gas/particle residence time versus bed rotating speed

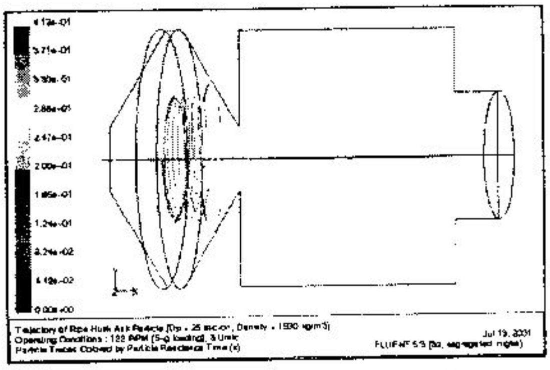

Figure 9: Trajectory of 25 μm ash particle in a RFB operating at 5-g loading (122 RPM), 3 U_{mfc}

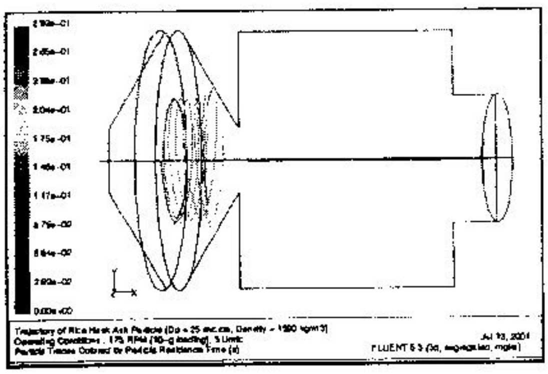

Figure 10: Trajectory of 25 μm ash particle in a RFB operating at 10-g loading (173 RPM), 3 U_{mfc}

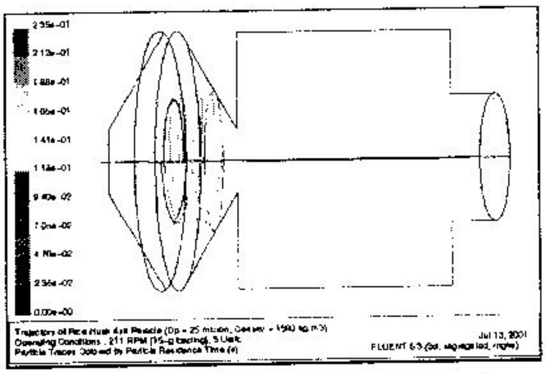

Figure 11: Trajectory of 25 μm ash particle in a RFB operating at 15-g loading (211 RPM), 3 U_{mfc}

Effect of air feed rates

The effect of air feed rates on the trajectories of rice husk ash particles were investigated by operating the horizontal RFB at 1 – 3 U_{mfc} while keeping the rotating speed constant at 15-g loading (211 RPM). Particles having a size of 10 μm were chosen since particle of this size exhibited significantly different trajectories due to the change in air feed rates. Similar to earlier cases, smaller sized particles (5 μm) were rapidly blown out from the primary chamber while larger sized particles (>25 μm) were either moving with the swirling flows in the primary chamber or were impacted towards the distributor.

Figure 12 and 13 clearly showed that particles of size 10 μm were captured and remained in circular orbits in the primary chamber. However, the circular orbit of the 10-μm particle has a fairly constant diameter (Figure 12). This, in part, was due to the increase in drag force with the increase in air feed rate, resulting in the net balancing between the centrifugal force (from the rotational effect) and drag force (from the fluidising fluid) on the particle. Lower drag force in the case of an air feed rate of 1 U_{mfc} resulted in a helical particle trajectory with a diverging trend (Figure 11). Air feed rate of 3 U_{mfc} was sufficient to blow out the 10-μm particle from the primary chamber (Figure 5). In addition, consistent with earlier explanation, the particle helical trajectory has a converging trend due to the much higher drag force from the air feed rate of 3 U_{mfc}.

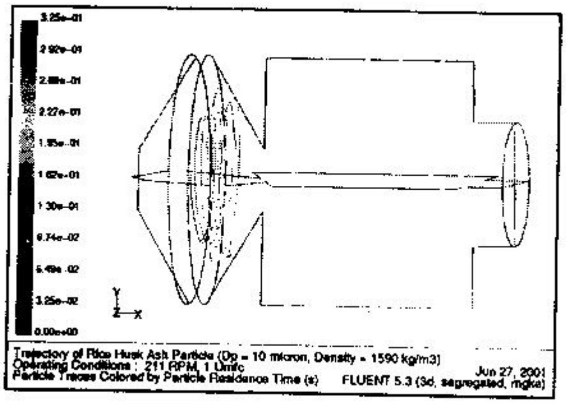

Figure 12: Trajectory of 10 mm ash particle in a RFB operating at 211 RPM, 1 U_{mfc} (@ room temp.)

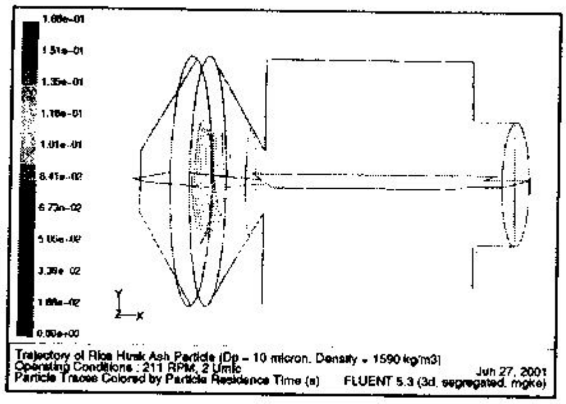

Figure 13: Trajectory of 10 mm ash particle in a RFB operating at 211 RPM, 2 U_{mfc} (@ room temp.)

CONCLUSIONS

Investigations on the effect of particle diameters on trajectories of rice husk ash in a horizontal RFB showed that particles with a size of 5 μm or less were rapidly blown out of the combustor. The 10-μm particle was caught in the re-circulating airflow regions just after the exit from the primary chamber. Particles of sizes in the range of 25 – 50 μm were retained in the primary chamber and moving in circular orbits. Larger-sized particles (1 mm) tended to move towards the distributor as the drag force from the fluidising gas is not sufficient to entrain them to the freeboard region.

The residence times of particles (25 μm) reduced as the bed rotating speeds were increased from 5-g loading to 15-g loadings. Due to the constraint that the bed be operated at more than 3 U_{mfc} (in order to establish turbulence conditions inside the bed), it was preferable for the bed to be operated at lower rotating speeds to increase the residence time of particles in the primary chamber. With the increase in fluidising air flow rates from 1 U_{mfc} to 2 U_{mfc}, the 10-μm particles were observed to be caught in circular orbits in the freeboard of the primary chamber. However, due to lower drag force of the gas in the case of 1 U_{mfc}, the helical trajectory of the particle tended to diverge as it moves towards the primary chamber exit. Higher airflow rate of 3 U_{mfc} generated sufficient drag force to blow the particle out of the primary chamber.

NOTATION

D_p	Particle diameter, (m)	ρ, ρ_f	Fluid density, (kg/m^3)
r	Radial position of the bed, (m)	ρ_p	Particle density, (kg/m^3)
r_i	Inner radius of the bed, (m)	μ_f	Fluid viscosity, (kg/m.s)
U_{mf}	Minimum fluidisation velocity, (m/s)	ω	Angular velocity, (rad/s)
U_{mfc}	Critical minimum fluidisation velocity, (m/s)		
U_{mfs}	Surface minimum fluidisation velocity, (m/s)		

ACKNOWLEDGEMENT

The authors acknowledged the IRPA (Intensification Research on Priority Areas) Grant Vot No. 72225 for sponsoring this research.

REFERENCES

[1] A. Haider and O. Levenspiel. *Drag Coefficient and Terminal Velocity of Spherical and Nonspherical Particles.* Powder Technology **58**, pp 63 – 70 (1989).

[2] H. S. Caram, Z. Efes and E. K. Levy. *Gas and particle motion induced by a bubble eruption at the surface of a gas fluidized bed.* AIChE Symposium Series **80** (234), pp 103 – 106 (1984).

[3] M. P. Subzwari. *Atmospheric and Pressurized Rotating Fluidized bed Combustion.* PhD Thesis, University of Sheffield (1983).

[4] M. Rozainee. *Incineration of Sludge Waste in a Novel Rotating Fluidized Bed,* PhD Thesis, University of Sheffield (1998).

[5] R. Chevray, Y. N. I. Chan and F. B. Hill. *Dynamics of bubbles and entrained particles in the rotating fluidized.* AIChE Journal **26**, No. 3, pp 390 – 397 (1980).

[6] S. A. Morsi and A. J. Alexander. *An Investigation of Particle Trajectories in Two-Phase Flow Systems.* J. Fluid Mech. **55(2)** pp 193 –208 (1972).

[7] S. T. Pemberton and J. F. Davidson. *Elutriation from fluidized beds – 1. Particle ejection from the dense phase into the freeboard.* Chemical Engineering Science **41**, pp 243 – 251 (1986).

APPENDIX 1 – MATHEMATICAL MODEL OF THE GAS PHASE

Conservation of mass (incompressible flow):- $\frac{\partial}{\partial x_i}(\rho u_i) = 0$

Ensemble-averaged momentum equation:-

$$\frac{\partial}{\partial x_j}(\rho u_i u_j) = \frac{\partial}{\partial x_j}\left\{\mu\left[\left(\frac{\partial u_i}{\partial x_j} + \frac{\partial u_j}{\partial x_i}\right) - \frac{2}{3}\frac{\partial u_l}{\partial x_l}\delta_{ij}\right]\right\} - \frac{\partial P}{\partial x_i} + \frac{\partial}{\partial x_j}\left(-\rho \overline{u_i' u_j'}\right)$$

The RNG (renormalization group) $\kappa - \varepsilon$ model:-

$$\frac{\partial}{\partial x_i}(\rho u_i \kappa) = \frac{\partial}{\partial x_i}\left(\alpha_\kappa \mu_t \frac{\partial \kappa}{\partial x_i}\right) + G_\kappa - \rho\varepsilon$$

$$\frac{\partial}{\partial x_i}(\rho u_i \varepsilon) = \frac{\partial}{\partial x_i}\left(\alpha_\varepsilon \mu_t \frac{\partial \varepsilon}{\partial x_i}\right) + C_{1\varepsilon} G_\kappa \frac{\varepsilon}{\kappa} - C_{2\varepsilon}\rho\frac{\varepsilon^2}{\kappa} - R$$

$$\mu_t = \mu_{t0} f\left(\alpha_s, \Omega, \frac{\kappa}{\varepsilon}\right) ; \quad \mu_{t0} = 0.0845\rho\frac{\kappa^2}{\varepsilon}$$

G_κ - generation of turbulent kinetic energy due to the mean velocity gradients; R - the effects of rapid strain and streamline curvature. For high Reynolds number, the values of the inverse Prandtl numbers for κ and ε (α_κ and α_ε) are approximately 1.393. The coefficients $C_{1\varepsilon}$ and $C_{2\varepsilon}$ are empirical constants having the following values:- $C_{1\varepsilon} = 1.42$ and $C_{2\varepsilon} = 1.68$